

Self-assembled Nanowire Arrays as Three-dimensional Nanopores for Filtration of DNA Molecules

Sakon RAHONG,^{*1,*2†} Takao YASUI,^{*2,*3†} Takeshi YANAGIDA,^{*4} Kazuki NAGASHIMA,^{*4}
Masaki KANAI,^{*4} Gang MENG,^{*4} Yong HE,^{*4} Fuwei ZHUGE,^{*4} Noritada KAJI,^{*2,*3} Tomoji KAWAI,^{*4}
and Yoshinobu BABA^{*2,*3,*5†}

^{*1} Institute of Innovation for Future Society, Nagoya University, Furo-cho, Chikusa, Nagoya, Aichi 464-8603, Japan

^{*2} FIRST Research Center for Innovative Nanobiodevices, Nagoya University, Furo-cho, Chikusa, Nagoya, Aichi 464-8603, Japan

^{*3} Department of Applied Chemistry, Graduate School of Engineering, Nagoya University, Furo-cho, Chikusa, Nagoya, Aichi 464-8603, Japan

^{*4} The Institute of Scientific and Industrial Research, Osaka University, 8-1 Mihogaoka, Ibaraki, Osaka 567-0047, Japan

^{*5} Health Research Institute, National Institute of Advanced Industrial Science and Technology (AIST), 2217-14 Hayashi-cho, Takamatsu 761-0395, Japan

Molecular filtration and purification play important roles for biomolecule analysis. However, it is still necessary to improve efficiency and reduce the filtration time. Here, we show self-assembled nanowire arrays as three-dimensional (3D) nanopores embedded in a microfluidic channel for ultrafast DNA filtration. The 3D nanopore structure was formed by a vapor-liquid-solid (VLS) nanowire growth technique, which allowed us to control pore size of the filtration material by varying the number of growth cycles. λ DNA molecules (48.5 kbp) were filtrated from a mixture of T4 DNA (166 kbp) at the entrance of the 3D nanopore structure within 1 s under an applied electric field. Moreover, we observed single DNA molecule migration of T4 and λ DNA molecules to clarify the filtration mechanism. The 3D nanopore structure has simplicity of fabrication, flexibility of pore size control and reusability for biomolecule filtration. Consequently it is an excellent material for biomolecular filtration.

Keywords Nanowire, 3D nanopore structure, biomolecular filtration

(Received December 12, 2014; Accepted January 14, 2015; Published March 10, 2015)

Introduction

Molecular filtration is a very important process in a wide range of chemical and biological disciplines from chemistry to biology. New advanced processes to filter and purify biological samples in a short time are required for bio-analytical separations such as that used in food inspection, healthcare diagnostics, environmental monitoring, *etc.* The conventional method by gel filtration chromatography can purify biomolecules by size and charge.^{1,2} However, this method is time consuming and also requires a large amount of the biological sample to be purified. Nanopore membranes, based on top-down approaches, have been developed to filter biomolecules.³⁻⁷ For example, Schultz and Beck³ proposed nanopore membranes, fabricated by track-etched processes,⁴ to study the hindered transportation theory for biomolecule filtration. In addition, Si-based ultrathin

nanopores integrated with a microfluidic system have been demonstrated; research in this area include those by Tong *et al.*⁶ who fabricated a 10 nm thick SiN nanosieve membrane with 10 - 25 nm diameter pores by a focused ion beam technique and Striemer *et al.*⁷ who fabricated a 10 nm thick Si nanopore membrane with 5 - 25 nm diameter pores and a 1 atm tolerance pressure across the membrane. However, nanopore membranes have not been widely used because polymer-based membranes have lower manufacturing costs.

Recently, nanostructures have been integrated into a microfluidic channel to enhance the filtration efficiency. After Volkmuth and Austin⁸ successfully observed and separated semiflexible polymer DNA molecules using a highly ordered microlithography array, many research groups started to develop highly ordered nanostructure devices for high throughput DNA filtration and purification; they include nanopillar,⁹ nanowall,¹⁰ nanochannel¹¹ and anisotropic nanofilter¹² arrays. These top-down approaches, however, require sophisticated facilities and a long device fabrication time using the electron beam lithography technique.

To overcome these issues for the top-down approaches, microfluidic channels have been filled with self-assembled particles

† To whom correspondence should be addressed.

E-mail: sakon.rahong@apchem.nagoya-u.ac.jp (S. R.); yasui@apchem.nagoya-u.ac.jp (T. Y.); babaymtt@apchem.nagoya-u.ac.jp (Y. B.)

as molecular sieving materials for molecular filtration; these devices include magnetic nanoparticles,¹³ core/shell nanoball structures¹⁴ and colloidal arrays of silica and polystyrene.¹⁵ These bottom-up approaches still have limitations in terms of their troublesome fabrication process that limits disposable usage of the devices. Recently, we presented bottom-up self-assembled nanowire structures as a sieving material embedded in a microfluidic channel for manipulation of long DNA molecules¹⁶ and for ultrafast DNA separation of a wide range of molecule sizes.¹⁷

Here we report an ultrafast DNA filtration by using self-assembled nanowire arrays embedded in a microfluidic channel as a sieving material. The self-assembled nanowire arrays can be fabricated by a vapor-liquid-solid (VLS) technique, which can prepare nanowire in nanoscale (10 – 50 nm) with high aspect ratio (>100) in microchannel, while the smallest diameter by the top down method is about 100 nm with an aspect ratio of about 10. The self-assembled nanowire also allows us to control the pore size by varying the number of nanowire growth cycles, which is not possible with other techniques. Furthermore, we can also reuse the three-dimensional (3D) nanopore structure filtration chip by cleaning with acid, which is difficult to achieve with other bottom-up methods. Our method offers simplicity and flexibility to fabricate the 3D nanopore structure embedded in the microfluidic channel for ultrafast filtration with high throughput.

Experimental

Fabrication of the self-assembled nanowire arrays embedded in the microfluidic channel

In order to fabricate the 3D nanopore structure devices, we have optimized a conventional photolithography process, electron beam lithography, and VLS growth technique for growth of the nanowires. A Cr layer (250 nm) was deposited on a quartz glass substrate by RF sputtering (SVC-700LRF, Sanyu Denshi). We employed the Cr layer as a hard mask for reactive ion etching (RIE). A positive photoresist (TSMR V50, Tokyo Ohka Kogyo Co.) was spin-coated on the substrate. Then, the microchannel pattern with a line width of 25 μm was created by a photolithography process. The Cr layer was etched by Cr etchant solution ($\text{H}_2\text{O}:\text{Ce}(\text{NH}_4)_2(\text{NO}_3)_6:\text{HClO}_4$, 85:10:5 %wt). After that, a microchannel was formed by RIE (RIE-10NR, Samco Co.) under CF_4 gas ambient. The microchannel depth was controlled at 2 μm . Via holes (1.5 mm diameter) for the inlet and outlet of the microfluidic system were drilled with an ultrasonic driller (SOM-121, Shinoda Co.). Then, we prepared the metal catalysts to define the spatial position of the nanowires within the microchannel. A 10 nm thick Cr layer was deposited within the microchannel. After that, a positive resist (ZEP520 A7, Zeon Corp.) was coated on the microchannel by spin coating, and then the rectangular pattern $25 \times 250 \mu\text{m}$ was prepared at the entrance of the separation channel by electron beam lithography (SPG-724, Sanyu Electron Co.). After developing the resist, the Cr layer pattern was removed with the Cr etchant solution. A 3 nm layer of Au metal catalyst was DC sputter-deposited within the microchannel for nanowire growth. The electron beam resist was lifted off by immersion in dimethylformamide, acetone and isopropanol, sequentially. The SnO_2 nanowires were grown in the microchannel by a pulse laser deposition (PLD) system. Details of the nanowire fabrication conditions can be found elsewhere.¹⁸⁻²¹ To prepare the 3D nanopore structure device, the Au catalyst particles were deposited along the nanowire by DC sputtering and the SnO_2

nanowires were grown cyclically using the PLD system six times. The Cr layer was removed by the Cr etchant solution. Then an SiO_2 layer was deposited onto the SnO_2 nanowires with the RF sputtering system to avoid the charge interaction between the nanowires and biomolecules. Finally, the microchannel was sealed using a fused silica cover glass (130 μm thick) according to the method described in literature.^{10,16,17}

DNA filtration and fluorescence measurement

To demonstrate the DNA filtration by the 3D nanopore structure, long DNA molecules, that is T4 DNA molecules (166 kbp) and λ DNA molecules (48.5 kbp) (both from Wako Pure Chemical Industries, Ltd.), were used. The DNA molecules were stained and mixed together with an intercalated fluorescence dye YOYO-1 (Invitrogen) at a dye base ratio of 1:15 for fluorescence observation. The final concentration of both DNA molecule sizes was 30 ng/ μL contained in buffer solution (TE buffer, pH 8.0, Wako Pure Chemical Industries, Ltd.). DNA filtration and fluorescence detection were done on an inverted fluorescent microscope (Eclipse TE-300, Nikon). A high voltage sequencer (HVS448-1500, Lab Smith) was used to apply the DC electric fields to control the DNA molecules and an Hg lamp was used to observe the fluorescently stained protein molecules. Fluorescence images were captured with an EB-CCD camera (C7190-43, Hamamatsu Photonics K.K.) through a 10 \times /1.40NA and a 100 \times /1.40NA objective lens (both

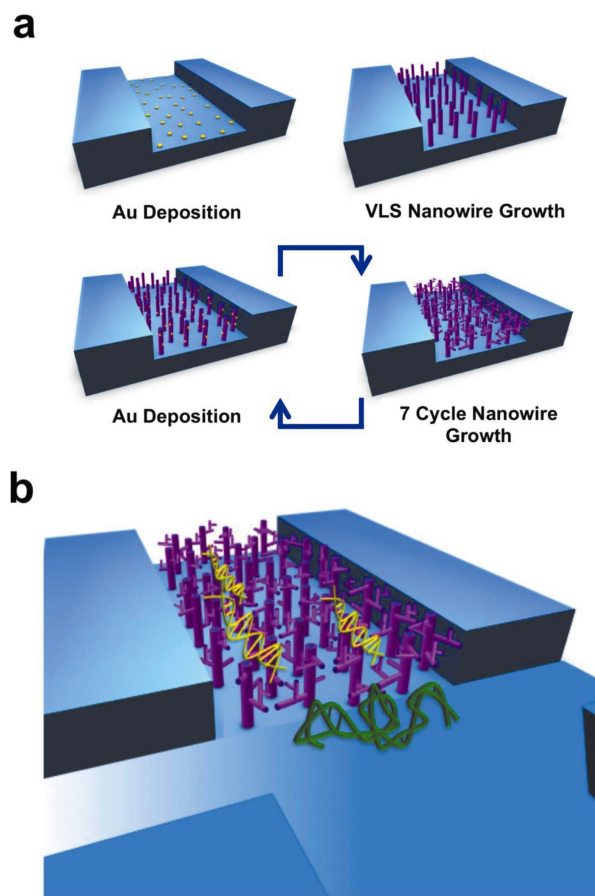


Fig. 1 Fabrication process of the self-assembled nanowire array as three-dimensional (3D) nanopores embedded in the microchannel. (a) Schematic of nanowire growth cycles in microchannels by the vapor-liquid-solid (VLS) technique. (b) Schematic of DNA filtration in the 3D nanopore structure.

from Nikon) for DNA filtration and single DNA molecule observation, respectively. The images were recorded on a DV tape (DSR-11, Sony) and then analyzed by image-processing software Image J (NIH, USA).

Results and Discussion

We developed the DNA filtration method using the 3D nanopore structure embedded in the microfluidic channel formed by the self-assembled nanowire arrays. According to our previous work,¹⁷ we prepared the nanowire embedded in the microchannel by varying the number of nanowire growth cycles from 1, 3 and 5 and the detection points were 1 and 3 mm from the junction. In this work, we increased the number of nanowire growth cycles to 7 times as illustrated in Fig. 1a. Our theory is that one type of biomolecule, which has a gyration size larger than the size of the nanopores, is trapped at the entrance while the second type with a smaller gyration size is passed through the nanopores under the applied high electric field (Fig. 1b). This concept can also be applied in high-throughput biomolecule trapping and pre-concentration.

The 3D nanopore structure embedded in the microfluidic channel was fabricated as illustrated in Fig. 2. The 3D nanopore structures were fabricated on a fused silica substrate (Fig. 2a) because of the high insulation property of the silica material. Figure 2b shows an SEM image of the SnO₂ nanowires, which formed the 3D nanopore structure at the entrance of the separation channel in the microfluidic system. The length of the nanowire area in the microchannel was designed as 100 μ m. A TEM image of the SnO₂/SiO₂ core/shell nanowire structure is shown in Fig. 2c. We prepared the SiO₂ shell layer to avoid an

electrostatic interaction between the nanowires and biomolecules. Figure 2d shows the SEM image for the 3D nanopore structure embedded in the microfluidic channel. Finally, the pore size distribution of the nanopores is shown in Fig. 2e.

T4 and λ DNA molecules were filtered by the 3D nanopore structure within 1 s under the DC electric field of 500 V/cm (Fig. 3 and Video clip S1 (Supporting Information)), and we could observe the filtration of T4- and λ -DNA molecules at the junction or at the entrance of the separation channel which can be achieved only in the 7-cycle nanowire growth. The time series fluorescence images were taken when the DNA mixture solution passed through the cross junction under the applied field as shown in Figs. 3a – 3f. We can see that λ DNA molecules started to migrate at the junction after the field was applied, while T4 DNA molecules still remained at the entrance of the separation channel. The electropherogram of T4 and λ DNA molecules was analyzed as shown in Fig. 3g as a function of the distance from the cross junction. It should be noted that λ DNA molecules could pass through the 3D nanopore structure, whereas T4 DNA molecules were hindered at the entrance.

One possible reason for the successful DNA filtration is the difference of the gyration radius of the selected DNA molecules. To confirm the effect of the gyration radius on DNA filtration, we observed the single DNA molecule migration behavior of T4 and λ DNA molecules in the 3D nanopore structure. The gyration radius of the λ DNA molecules (520 nm) was about 10 times larger than the pore size distribution of the 3D nanopore structure (5 – 50 nm); nevertheless the migration mechanism of the λ DNA molecules showed the biased reptation (Video clip S2, Supporting Information). The λ DNA molecules collided with the 3D nanopores structure under the applied DC electric field, and then, the λ DNA molecules unhooked and elongated

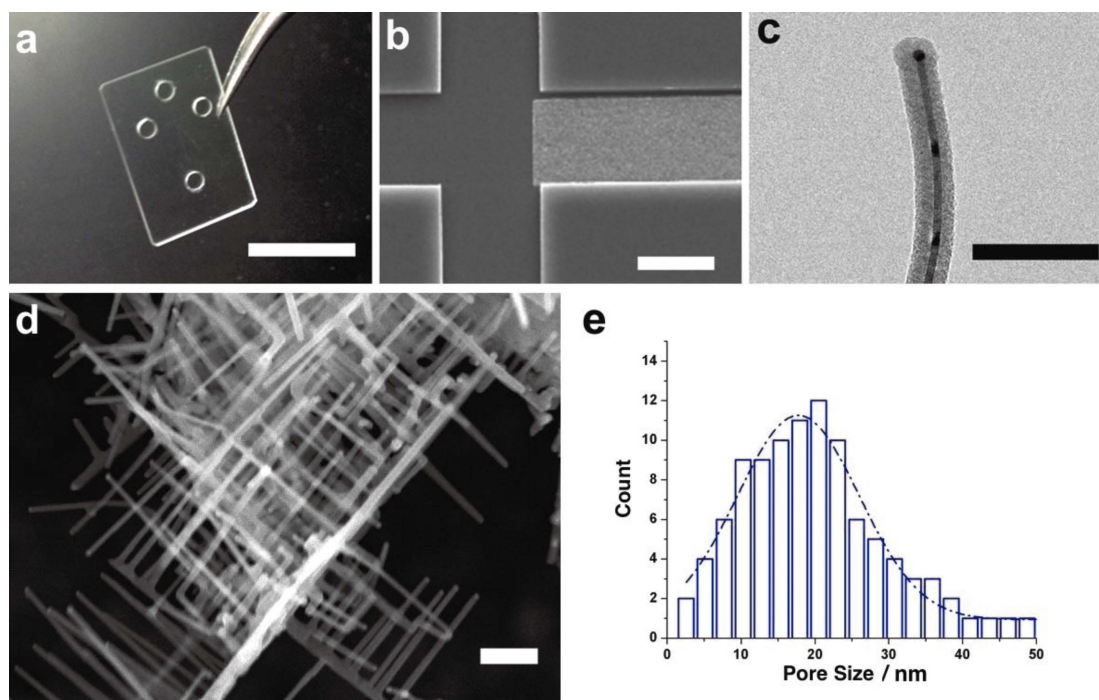


Fig. 2 3D nanopore structure embedded in the microchannel. (a) Photograph of the 3D nanopore structure embedded in the device, scale bar = 10 mm. (b) SEM image of the 3D nanopore structure embedded in the microfluidic channel, scale bar = 20 μ m. (c) TEM image of the SnO₂/SiO₂ nanowire core/shell structure, scale bar = 100 nm. (d) SEM image of the 3D nanopore structure, scale bar = 100 nm. (e) Pore size distribution of the 3D nanopore structure.

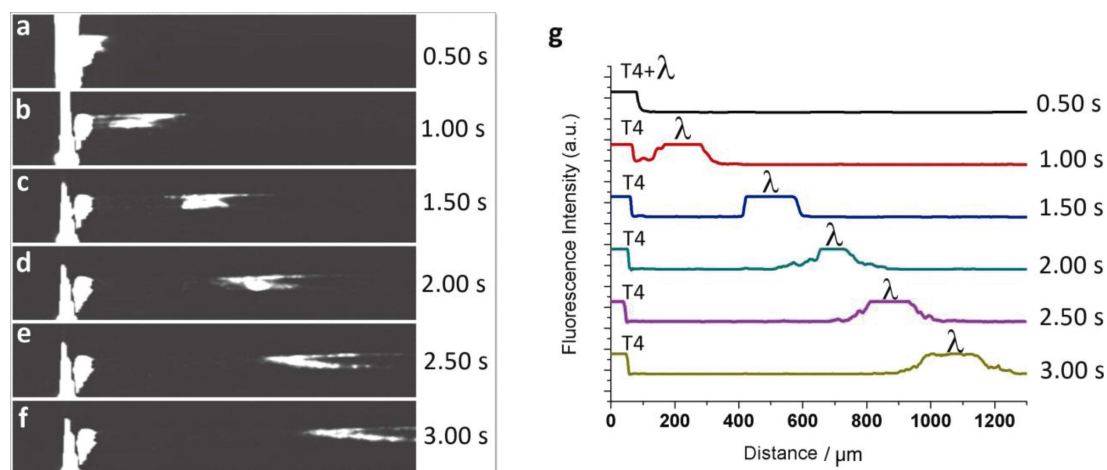


Fig. 3 T4 and λ DNA molecules separated by filtration in the 3D nanopore structure. (a – f) The time series fluorescence images of T4 and λ DNA molecules during filtration under a DC electric field of 500 V/cm. (g) Tracking time series of λ DNA molecule filtration in the 3D nanopore structure.

before being released from the nanowire. On the other hand, the T4 DNA molecules that migrated to the 3D nanopore structure stopped at the entrance without elongation (Video clip S3, Supporting Information) despite the fact that the gyration radius of the T4 DNA molecules was just 20 times larger than the pore size distribution. Such a size difference seemed to cause the two behaviors, trapping at and passing through the 3D nanopore structure.

Another possible scenario involves the mobility difference between T4 and λ DNA molecules in the 3D nanopore structure. We used the fitting curve for the DNA mobility (Fig. S1, Supporting Information) to measure the mobility of T4 and λ DNA molecules in the 3D nanopore structure. The mobility values of T4 and λ DNA molecules were $0.6723 \times 10^{-5} \text{ cm}^2/\text{Vs}$ and $1.0350 \times 10^{-5} \text{ cm}^2/\text{Vs}$, respectively. The mobility difference might be a factor responsible for the DNA filtration; the λ DNA molecules could penetrate into the 3D nanopore structure faster than the T4 DNA molecules could. According to the electrophoretic mobility difference of the DNA molecules in the 3D nanopore region (Fig. S1), we may also estimate the filtration size of the DNA molecules.

We could also observe the biomolecule filtration in a short time because the 3D nanopore structure allows us to apply a higher electric field than in gel chromatography. The $\text{SnO}_2/\text{SiO}_2$ nanowire core/shell, which forms the hard gel-like 3D nanopore structure,¹⁶ has a rigidity (Young's modulus $\approx 100 \text{ GPa}$)²² that is higher than that of agarose gel or poly acrylamide gel (Young's modulus $\approx 0.1 - 1 \text{ MPa}$).²³ The biomolecules migrate in the rigid network as if they were in a free solution environment, whereas the biomolecule migration in a soft material network is hindered by the elasticity of the matrix material. However, the scenarios based on differences of the DNA gyration radius and the DNA electrophoretic mobility, as well as the stiffness of the 3D nanopores structure cannot clearly explain the present results. The ultrafast filtration of DNA molecules in the 3D nanopore structure must be more complicated and theoretical and experimental studies are still required to clarify the actual filtration mechanism. In the near future, we expect that the 3D nanopore structure will be applied to trap cells for single-cell analysis or applied for biomolecule pre-concentration with high throughput in a short time.

Conclusions

In summary, we have demonstrated the filtration of T4 and λ DNA molecules within 1 s using the 3D nanopore structure embedded in the microfluidic channel as a sieving material. The $\text{SnO}_2/\text{SiO}_2$ core/shell nanowire structure formed the 3D nanopore structure embedded in the microchannel, and the pore size of the structure was controlled by increasing the number of nanowire growth cycles. λ DNA molecules could migrate under the biased reptation mechanism, but the larger T4 DNA molecules were hindered at the entrance of the 3D nanopore structure. Further experimental and theoretical studies are required to enhance knowledge of the ultrafast filtration. We offer the developed flexible platform to filter biomolecules with high throughput in a short time and to bring researchers closer to its integration with other micro-nanostructures for purification of biomolecules.

Acknowledgements

This research was supported by the Cabinet Office, Government of Japan and the Japan Society for the Promotion of Science (JSPS) through the Funding Program for World-Leading Innovative R&D on Science and Technology (FIRST Program); Nanotechnology Platform Program (Molecule and Material Synthesis) of the Ministry of Education, Culture, Sports, Science and Technology (MEXT), Japan; the JSPS Grant-in-Aid for Scientific Research (A) 24241050; and the JSPS Grant-in-Aid for Young Scientists (B) 25790028. Thanks are extended to Dr. H. Yukawa and Dr. D. Onoshima, both of Nagoya University, for valuable discussions.

Supporting Information

Video clip S1: Video clip of DNA filtration between T4 DNA and λ DNA by the 3D nanopore structure under an applied DC electric field of 500 V/cm. Video clip S2: Video clip of a single λ DNA molecule that migrated into the 3D nanopore structure under an applied DC electric field of 500 V/cm. Video clip S3:

Video clip of a single T4 DNA molecule that migrated into the 3D nanopore structure under an applied DC electric field of 500 V/cm. Fig. S1: The fitting curve for electrophoretic mobility of DNA molecules in the 3D nanopore structure under an applied DC electric field of 500 V/cm. This material is available free of charge on the Web at <http://www.jsac.or.jp/analsci/>.

References

1. C. R. J. Ruthven, T. Bernhard, B. Memorial, and Q. Charlotte, *Biochem. J.*, **1954**, *62*, 665.
2. J. Porath and P. Flodin, *Nature*, **1959**, *183*, 1657.
3. R. E. Beck and J. S. Schultz, *Science*, **1970**, *170*, 1302.
4. R. L. Fleischer, H. W. Alter, S. C. Furman, P. B. Price, and R. M. Walker, *Science*, **1972**, *178*, 255.
5. W. M. Deen, *AIChE J.*, **1987**, *33*, 1409.
6. H. D. Tong, H. V. Jansen, V. J. Gadgil, C. G. Bostan, E. Berenschot, C. J. M. van Rijn, and M. Elwenspoek, *Nano Lett.*, **2004**, *4*, 283.
7. C. C. Striemer, T. R. Gaborski, J. L. McGrath, and P. M. Fauchet, *Nature*, **2007**, *445*, 749.
8. W. Volkmuth and R. Austin, *Nature*, **1992**, *358*, 600.
9. N. Kaji, Y. Tezuka, Y. Takamura, M. Ueda, T. Nishimoto, H. Nakanishi, Y. Horiike, and Y. Baba, *Anal. Chem.*, **2004**, *76*, 15.
10. T. Yasui, N. Kaji, R. Ogawa, S. Hashioka, M. Tokeshi, Y. Horiike, and Y. Baba, *Anal. Chem.*, **2011**, *83*, 6635.
11. S. Pennathur, F. Baldessari, J. G. Santiago, M. G. Kattah, J. B. Steinman, and P. J. Utz, *Anal. Chem.*, **2007**, *79*, 8316.
12. J. Fu, R. B. Schoch, A. L. Stevens, S. R. Tannenbaum, and J. Han, *Nat. Nanotechnol.*, **2007**, *2*, 121.
13. P. S. Doyle, J. Bibette, A. Bancaud, and J.-L. Viovy, *Science*, **2002**, *295*, 2237.
14. M. Tabuchi, M. Ueda, N. Kaji, Y. Yamasaki, Y. Nagasaki, K. Yoshikawa, K. Kataoka, and Y. Baba, *Nat. Biotechnol.*, **2004**, *22*, 337.
15. Y. Zeng and D. J. Harrison, *Anal. Chem.*, **2007**, *79*, 2289.
16. T. Yasui, S. Rahong, K. Motoyama, T. Yanagida, Q. Wu, and N. Kaji, *ACS Nano*, **2013**, *7*, 3029.
17. S. Rahong, T. Yasui, T. Yanagida, K. Nagashima, M. Kanai, A. Klamchuen, G. Meng, Y. He, F. Zhuge, N. Kaji, T. Kawai, and Y. Baba, *Sci. Rep.*, **2014**, *4*, 5252.
18. A. Klamchuen, T. Yanagida, M. Kanai, K. Nagashima, K. Oka, S. Rahong, M. Gang, M. Horprathum, M. Suzuki, Y. Hidaka, S. Kai, and T. Kawai, *Appl. Phys. Lett.*, **2011**, *99*, 193105.
19. G. Meng, T. Yanagida, K. Nagashima, T. Yanagishita, M. Kanai, K. Oka, A. Klamchuen, S. Rahong, M. Horprathum, B. Xu, F. Zhuge, Y. He, H. Masuda, and T. Kawai, *RSC Adv.*, **2012**, *2*, 10618.
20. G. Meng, T. Yanagida, K. Nagashima, H. Yoshida, M. Kanai, A. Klamchuen, F. Zhuge, Y. He, S. Rahong, X. Fang, S. Takeda, and T. Kawai, *J. Am. Chem. Soc.*, **2013**, *135*, 7033.
21. G. Meng, T. Yanagida, H. Yoshida, K. Nagashima, M. Kanai, F. Zhuge, Y. He, A. Klamchuen, S. Rahong, X. Fang, S. Takeda, and T. Kawai, *Nanoscale*, **2014**, *6*, 7033.
22. S. Barth, C. Harnagea, S. Mathur, and F. Rosei, *Nanotechnology*, **2009**, *20*, 115705.
23. K. S. Kolahi, A. Donjacour, X. Liu, W. Lin, R. K. Simbulan, E. Bloise, E. Maltepe, and P. Rinaudo, *PLoS One*, **2012**, *7*, e41717.